IMPROVING THE DENSITY OF COHERENT PIXELS IN DINSAR WITH MULTIPLE IMAGES TECHNIQUES EMPLOYING BAND AND POLARIMETRIC COMBINATIONS FOR DEFORMATION MONITORING

P. Blanco-Sánchez, L. Pipia, F Pérez and R. Arbiol

Remote Sensing Department
Institut Cartogràfic de Catalunya (ICC)
Parc de Montjuïc, s/n, 08038 Barcelona, Spain
pablo.blanco@icc.cat

Abstract—**The appearance of new SAR missions opens new possibilities to increase the amount of useful information which serve as input to the Multi Image Differential Interferometry (MI DInSAR) techniques and brings complementarity to the already successful C-band missions as ESA's ERS and ENVISAT. In the frame of deformation monitoring, L-C band combination strategies are here investigated. L-band coherence enhancement in rural areas is addressed, allowing information retrieval on areas that would be inaccessible at C-band. Furthermore, PALSAR polarimetric channels combination is investigated in order to increase the number of pixels from whom deformation values can be extracted.**

Coherence, DInSAR, polarimetry, subsidence, terrain deformation

I. INTRODUCTION

During the past years, Multiple Images DInSAR (MI DInSAR) techniques have been widely developed [1-4] revealing to be a reliable tool for deformation monitoring. These techniques are able to provide the temporal deformation pattern of the studied area minimizing the effects of atmospheric artifacts. The upcoming of new SAR sensors expands MI DInSAR capabilities towards a more complete characterization of the motion information of the studied area.

In particular, L band ALOS-PALSAR present two important features which can be foreseen as complementary to the existent list of SAR sensors. These are its 1280 MHz working frequency and its polarimetric capabilities. Keeping in mind the final scope of retrieving temporal deformation from the studied areas, ALOS-PALSAR benefits and combining strategies with other band working sensors are here investigated. A test area where different deformation phenomena are taken place has been chosen. Correspondingly, a stack of PALSAR and ASAR interferograms have been created and different tests have been done among them. The employed data is described in section II.

Scattering mechanism depend, among others, on the wavelength of the employed signal. This makes L-band especially interesting over vegetated areas as, in opposition to C-band, penetration allows to study the underneath canopy surface behaviour. In coherence terms this should provoke a coherence improvement and access to non coherent areas in C-band images. In order to validate this, coherence performances are studied over the PALSAR and ASAR stacks. Therefore, when moving into a MI DInSAR frame, an increment of the number of useful points should be expected. This study is performed in section III.

Before applying MI DInSAR techniques, some conclusions can be already obtained by investigating the PALSAR and ASAR differential interferograms corresponding to a wide and strong (-30 cm/y) subsidence movement caused by mining activity. This is done in section IV.

PALSAR is capable to provide full polarimetric images. The employed PALSAR stack accounts for HH and HV images. Therefore, efforts are addressed to take profit of both channels to increase the density of useful pixels. Employing coherence as a scattering stability indicator, a HH and HV channel combination on the stack of interferograms is also proposed. The corresponding linear velocity maps of an area suffering a long term (-2 cm/y) and localized subsidence movement are generated. This is addressed in section V

Finally, conclusions and future work are exposed in section VI.

II. AVAILABLE DATA

The test area is located in the Bages region in Catalonia (Spain). The ALOS-PALSAR FBS and FBD coverage corresponds to path 660 and frames 820. The ENVISAT-ASAR coverage corresponds to track 244 and frame 837 (in green). In this area, several deformation episodes have been reported, mainly caused by mining activities.

The spatio-temporal distribution of the PALSAR and ASAR interferogram are depicted in Fig.1 .The nodes represent the images and the arcs, the interferograms. The ASAR stack is composed of 23 interferograms out of 10 (black) images from

Proc. 'Fringe 2009 Workshop', Frascati, Italy,
30 November – 4 December 2009 (ESA SP-677, March 2010)

the last quarter of 2005 to the last quarter of 2008 with a maximum spatial baseline of 500 m. The PALSAR stack is composed of 13 interferograms out of 6 FBD (blue) images going from mid 2007 to mid 2009, with a maximum spatial baseline of 1400 m. A selection on the ENVISAT data could be done so only those [2007, 2009] images and their corresponding interferograms (in correspondence to PALSAR) had been included in the phase analysis. Nevertheless, it has been preferred to take profit of the whole dataset so a more reliable statistic is at least available for ASAR.

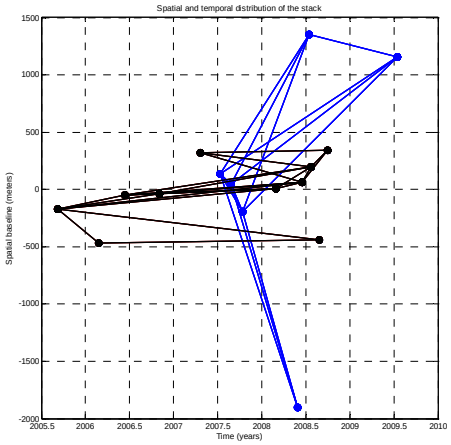

Figure 1. ASAR (black) and PALSAR (blue) interferograms distribution.

III. C BAND VS. L BAND. COHERENCE BEHAVIOUR

Employing the described ASAR and PALSAR HH and HV interferograms stacks, their mean coherence maps are computed over the area of interest (Figs. 2, 3 and 4 respectively). The studied area comprises both urban and rural areas. Multi-look factor is 10 az. x 2 rg. for ASAR and 6 az. x 2 rg. for PALSAR yielding a pixel size of 40 az. x 40 gr. rg. and 30 x 20 correspondingly.

According to the results, PALSAR coherence is significantly increased in the rural areas compared to the ASAR coherence map as expected due to the penetration of longer wavelength on moderate vegetation. Urban areas remain coherent for both sensors. As commented, both temporal distributions are different and the ASAR set includes larger temporal baselines interferograms. Therefore, temporal decorrelation may be higher in the ASAR set. Nevertheless, when comparing mean coherence maps from similar periods and temporal baselines, the aforementioned behaviour is also reproduced.

The histograms of the mean coherence maps are computed and depicted in Fig.5. Here, PALSAR histograms are computed separately employing the HH and the HV interferograms. Confirming the mean coherence maps results, PALSAR coherence values are higher than ENVISAT's. Furthermore, HH channel is slightly higher than HV.

From these results, two main conclusions can be extracted. First, L band brings coherent information in areas where C band does not. Second, both HH and HV channels are comparable in terms of phase quality, so strategies should be developed to combine both channels for deformation extraction purposes.

To confirm the obtained results, more PALSAR images are demanded, so further tests will be done in the future.

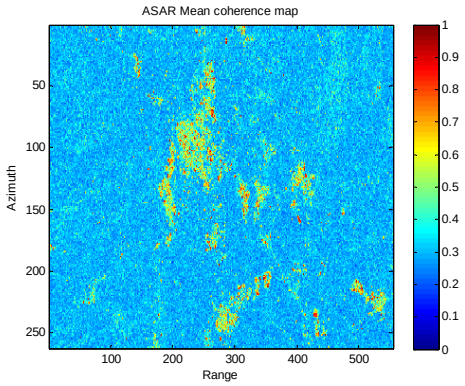

Figure 2. ASAR mean coherence map.

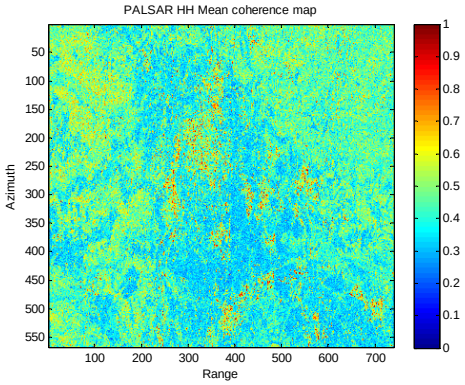

Figure 3. PALSAR HH mean coherence map.

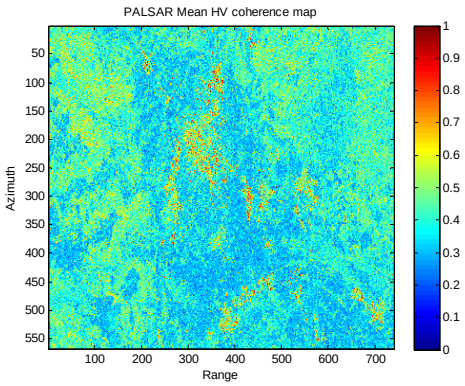

Figure 4. PALSAR HV mean coherence map.

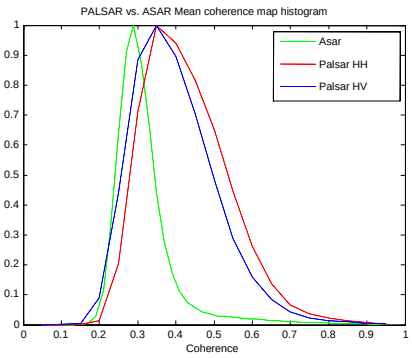

Figure 5. ASAR (green), PALSAR HH (red) and PALSAR HV (blue) mean coherence maps histograms.

IV. DInSAR RESULTS

In the test area, fast and extensive movements were detected in previous studies [4] employing ASAR images, caused by subterranean mining works in the area. These are significant enough to be clearly detectable despite of the atmospheric artefacts. Nevertheless, as they are located at vegetated areas, PALSAR phase is investigated to test quality enhancement where C band fringes were masked.

Picked out of the PALSAR and ASAR interferograms stacks, two 2008 PALSAR interferograms of the deformation area are depicted Fig.6 in the upper row (46 days and 92 days temporal baselines). ENVISAT highest quality interferograms in 2008 are depicted in the lower row (35 days and 105 days temporal baseline). The detected movement magnitude is larger than -30 cm/year PALSAR fringes are better defined than ASAR, so the area monitoring can be improved by combining both sources of information.

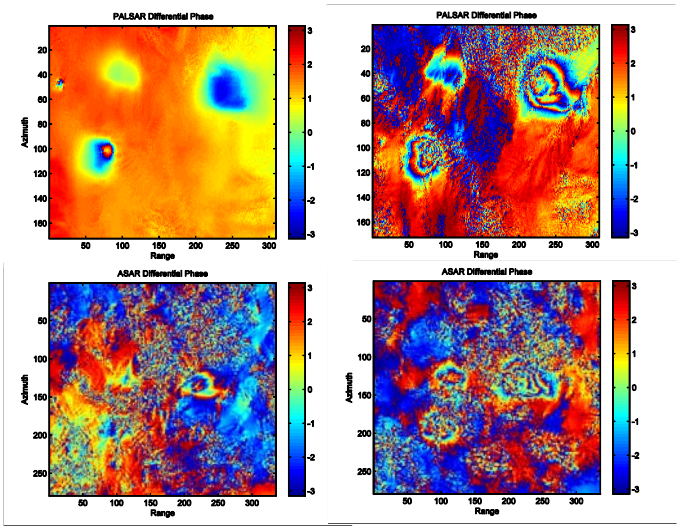

Figure 6. Deformation fringes (< -30 cm/year) generated by mine activities seen by PALSAR (first row) and ASAR (second row).

Both band results are therefore complementary. The longer the wavelength the higher the sensitivity to the movement, therefore low movements would be hard to detect with L band but not in C-X band. On the contrary, on the same temporal span, quick movement will present more unwrapping problems in terms of number of fringes and decorrelation in higher frequencies.

V. POLARIMETRIC COMBINATION FOR COHERENT POINTS DENSITY ENHANCEMENT

Prior to apply the MI DInSAR algorithm, it is mandatory to select the quality pixels among the stack of interferograms. In our approach quality pixels are those who overcome a mean threshold coherence value. In order to take profit of both ALOS HH and HV channels a strategy is proposed. The objective is to increase the number of useful points where deformation information could be extracted.

The simple combination depicted in Fig.7 is proposed. For each pixel it is investigated whose channel yield the maximum mean coherence value max(E[HH], E[HV]) along the stack. Therefore a new mean coherence map can be calculated where each pixel will show that max(E[HH], E[HV]) value. Correspondingly a quality pixel map is obtained by imposing a threshold value on the new mean coherence map. In the same way, a new interferogram stack is conformed to be the input of our MI DInSAR algorithm. The phase of each pixel at each interferogram will correspond to the phase value of the polarization channel at that interferogram which has shown the maximum mean coherence value for that pixel.

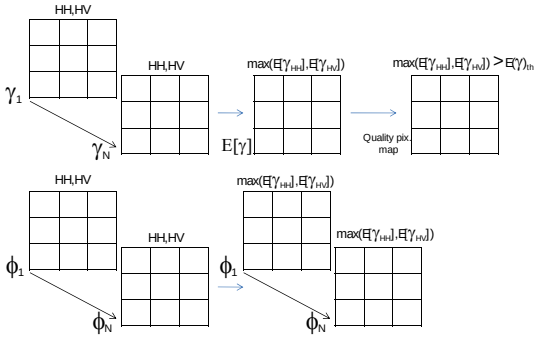

Figure 7. Combination of HH and HV PALSAR channels for increasing the number of selected pixels and improve the phase information quality.

After imposing a mean coherence threshold value of 0.6, the selected pixels are depicted separately in Figs. 8 and 9 for those whose mean coherence value is larger in HH than HV and vice-versa. In each case the number of selected pixels is 16336 and 6621 correspondingly. This means that the new interferogram stack would account with a number of selected pixels equal to the summation of these values.

Therefore it is remarked that not only new pixels that would not be selected when working with FBS images are taken into account, but also it is improved the phase quality of some that would have been chosen if only working with single pol images.

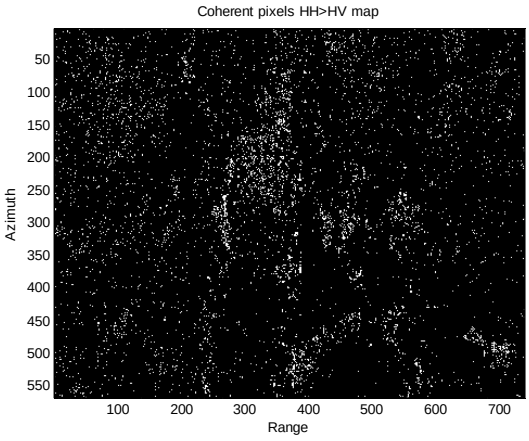

Figure 7. Selected pixels are those whose mean coherence is higher in the HH stack than in the HV stack.

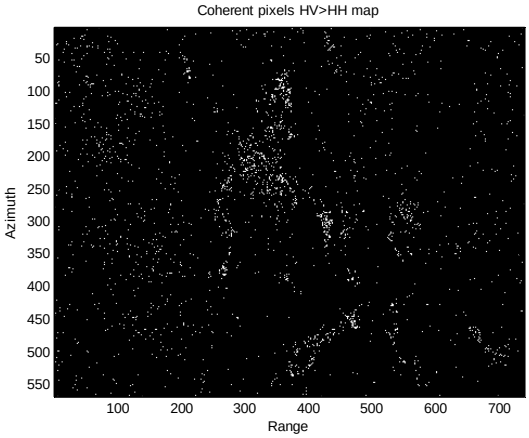

Figure 8. Selected pixels are those whose mean coherence is higher in the HV stack than in the HH stack.

VI. MI DINSAR DEFORMATION RESULTS

Once having described the HH and HV combination method, the MI DInSAR processor developed at the ICC [4] is applied to the ASAR stack and the PALSAR HH, HV combination stack over the city of Sallent.

The city of Sallent presents a long-term subsidence movement in one of its neighbourhoods, caused by salt dissolution. ASAR and PALSAR HH stacks are processed with the ICC MI DInSAR algorithm. The selected points are those whose mean coherence value exceeds 0.4 in ASAR and 0.55 in PALSAR HH, HV combination. Due to the lower number of PALSAR interferograms coherence threshold is higher to ensure quality deformation results.

The Sallent geocoded linear velocity maps of ASAR and the HH and HV PALSAR combination of Sallent are depicted in Fig. 9 (left and right correspondingly). Even though it is possible to retrieve temporal series from PALSAR, the low number of images has prevented to do so.

Taking PALSAR quantities as approximate (due to the low number of images and interferograms employed) and assuming that temporal spans are not identical, three main conclusions can be extracted. In general, deformation behaviour is similar, PALSAR allows access to C-band non-coherent areas and a simple polarimetric channel is suitable for increasing the number and quality of coherent points which is helpful to give a more complete deformation interpretation.

Again, more images are needed to extract more solid conclusions.

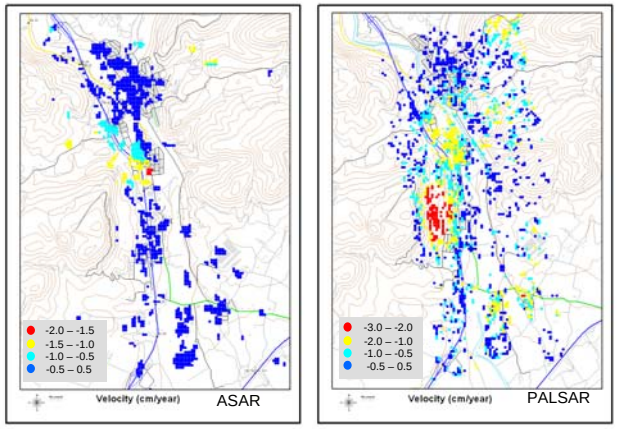

Figure 9. Linear velocity map of Sallent obtained from the ASAR stack (right) and the combination of HH and HV PALSAR channel (left). stack (left).

VII. CONCLUSIONS

Band and polarimetric data combination or deformation monitoring have been investigated. L-band coherence enhancement (mainly in rural areas) as well as its polarimetric capabilities lead to an increment of useful points and, therefore, access to new deformation information. In this sense, L and C band results have to be envisaged as complementary. More PALSAR images are needed to extend these studies. Furthermore, full-pol images have to be included, as more optimized combination will be allowed. Combination optimization of the polarimetric channels as well as the L and C (and X) band data represents a mandatory issue for a more complete deformation monitoring characterization..

ACKNOWLEDGMENTS

This work has been sponsored by JAXA and ESA under ALOS ADEN AOALO.3655

REFERENCES

[1] Pablo Blanco-Sanchez, Jordi J. Mallorquí, Sergi Duque, and Daniel Monells, “The Coherent Pixels Technique (CPT): An Advanced DInSAR Technique for Nonlinear Deformation Monitoring,” Pure Appl. Geophys., No. 165, pp. 1167-1194, 2008.

[2] A. Ferretti, C. Prati, F. Rocca, “Permanent scatterers in SAR interferometry”, IEEE Trans. on Geoscience and Remote Sensing, Vol. 39, No 1, pp. 8-30, 2001.

[3] P. Berardino, G. Fornaro, R. Lanari, E. Sansosti, “A New Algorithm for Surface Deformation Monitoring Based on Small Baseline Differential

Interferograms", IEEE Trans. on Geoscience and Remote Sensing, Vol. 40, No. 11, pp. 2375-2383, 2002.

[4] Mora,O., Arbiol,R., Palà,V, "ICC's Project for DInSAR Terrain Subsidence Monitoring of the Catalonian Territory", Proceedings of IGARSS 2007,Barcelona.